J. Astrophys. Astr. (2019) 40:42
https://doi.org/10.1007/s12036-019-9608-z

Radio pulsar sub-populations (I): The curious case of nulling pulsars

SUSHAN KONAR[1,*] and UDDEEPTA DEKA[2]

[1]NCRA-TIFR, Pune 411007, India.
[2]Department of Physics and Astrophysics, University of Delhi, Delhi 110007, India.
*Corresponding author. E-mail: sushan@ncra.tifr.res.in

MS received 24 May 2019; accepted 11 September 2019

Abstract. About ∼200 radio pulsars have been observed to exhibit nulling episodes – short and long. We find that the nulling fraction of a pulsar does not have any obvious correlation with any of the intrinsic pulsar parameters. It also appears that the phenomenon of nulling may be preferentially experienced by pulsars with emission coming predominantly from the polar cap region, and also having extremely curved magnetic fields.

Keywords. Radio pulsar—nulling—death-line.

1. Introduction

Fifty years of observations have yielded ∼3000 neutron stars, with diverse characteristic properties, which fall into three major categories, namely (a) the rotation powered, (b) the accretion powered, and (c) the internal-energy powered neutron stars; according to their mechanisms of energy generation (Kaspi 2010; Konar 2013; Konar *et al.* 2016; Konar 2017). Radio pulsars, which belong to the category of rotation powered pulsars (RPP), are strongly magnetized rotating neutron stars (mostly isolated or in non-interacting binaries) characterized by their short spin periods ($P \sim 10^{-3} - 10^{2}$ s) and large inferred surface magnetic fields ($B \sim 10^{8} - 10^{15}$ G). Powered by the loss of rotational energy, they emit highly coherent radiation (typically spanning almost the entire electromagnetic spectrum) which are observed as narrow emission pulses. The abrupt cessation of this pulsed emission for several pulse periods, observed in a small subset of radio pulsars, is known as the phenomenon of nulling - noticed for the first time by Backer (1970). Since then, close to two hundred radio pulsars have been observed to experience nulling. In this context, it needs to be noted that most of the ∼2600 radio pulsars are neither monitored regularly, nor are searched for the presence of nulling. This would imply that two hundred is just a lower limit to the actual number of nulling pulsars. On the other hand, presence of nulling may also depend on the sensitivity of a given telescope (e.g. a telescope with a low sensitivity may consider a pulsar to be nulling when a similar (or same) pulsar might be detected in weak emission by an instrument with higher sensitivity), giving rise to an over-estimate of the number of nulling pulsars.

In general, two parameters are used to quantify the phenomenon of nulling:

1. the nulling fraction (NF) – the total percentage fraction of pulses without detectable emission; and,
2. the null length (NL) – the duration of a given nulling episode.

Both NF and NL are observed to span a wide range - while NF ranges from just a few to more than 90%, NL can go from the simple case of single pulse nulls to the extreme situation of complete disappearance of pulsed emission for as long as a few years. Even though most pulsars are known to be characterised by a single value of NF (see the tables in the Appendix. for some contrary cases), neither NF nor NL can uniquely describe the behaviour of a nulling pulsar. It is well known that NL not only varies from one pulsar to another, but also from episode to episode for a given pulsar (Young *et al.* 2012). Moreover with increasing data it is becoming evident that two different pulsars having very different values of NL and totally different nulling behaviour can have the same average value of NF (Gajjar *et al.* 2012). For example, the long quiescent states of intermittent pulsars are in stark contrast to the longest known quiescence

Published online: 11 October 2019

times of ordinary nulling pulsars, i.e., they differ in their nulling timescale by about five orders of magnitude - even when the NF values are similar for both cases.

A detailed discussion on different types of nulling behaviour can be found in Gajjar (2017) and references therein. Despite the wide variation in NL, the population does render itself to a broad classification, depending on the nature of nulling, as follows:

1. Classical Nuller (CN) – pulsars with mostly single (or just a few) pulse nulls, for example - $J0837-4135$, J2022+5154 (Gajjar *et al.* 2012);
2. Intermittent Nuller (IN) – NL is longer, could be up-to a few hours combined with a longer period of activity, for example - $J1717-4054$ (Johnston *et al.* 1992), $J1634-5107$ (O'Brien *et al.* 2006), $J1709-1640$ (Naidu *et al.* 2018);
3. Intermittent Pulsar (IP) – NL can vary from days to years, for example - J1933+2421 (Kramer *et al.* 2006a), J1832+0029 (Lorimer *et al.* 2012), J1910+0517 & J1929+1357 (Lyne *et al.* 2017);
4. Rotating Radio Transient (RRAT) - Discovered in 2006, the RRATs are characterised by their sporadic single pulse emissions (McLaughlin *et al.* 2006). Whether these can be considered to be part of the nulling fraternity is a contentious issue, which we plan to take up in a later study (Konar 2019).

The phenomenon of nulling is usually observed to be associated with other emission features, like the *drifting of sub-pulses* and *mode changing* (Wang *et al.* 2007). Certain other behavioural changes have also been seen in nulling pulsars. In J1933+2421 the spin-down rate has been observed to decrease in the inactive phase compared to the active phase, suggestive of a depletion in the magnetospheric particle outflow in the quiescent phase of the pulsar (Kramer *et al.* 2006b; Lyne *et al.* 2009). An exponential decrease in the pulse energy during a burst has also been seen in certain nulling pulsars (Rankin & Wright 2008; Bhattacharyya *et al.* 2010; Li *et al.* 2012; Gajjar *et al.* 2014). Interestingly, nulling behaviour has not yet been observed in a millisecond pulsar (Rajwade *et al.* 2014), even though the cumulative study of this class of pulsars is close to 10^3 years.

In general, two different classes of models are invoked to explain the phenomenon of nulling, explaining it to arise from (a) intrinsic causes or (b) geometrical effects. Some of the models attributing nulling to an intrinsic cause are as follows:

- the loss of coherence conditions (Filippenko & Radhakrishnan 1982);
- a complete cessation of primary particle production (Kramer *et al.* 2006b; Gajjar *et al.* 2014);
- changes in the current flow conditions in the magnetosphere (Timokhin 2010);
- a transition to a much weaker emission mode (or an extreme case of mode changing) (Esamdin *et al.* 2005; Wang *et al.* 2007; Timokhin 2010; Young *et al.* 2014);
- time-dependent variations in an emission 'carousel model' (Deshpande & Rankin 2001; Rankin & Wright 2007); etc.

On the other hand, a variety of geometrical effects have also been suggested to explain nulling, like -

- the line-of-sight passing between emitting subbeams giving rise to 'pseudo-nulls' (Herfindal and Rankin 2007, 2009; Rankin & Wright 2008);
- occurrence of various unfavourable changes in the emission geometry (Dyks *et al.* 2005; Zhang *et al.* 2007).

Detailed investigations of the nulling behaviour of individual pulsars and theoretical modeling of this phenomenon have been undertaken by many groups (Ritchings 1976; Rankin 1986; Biggs 1992; Wang *et al.* 2007; Gajjar *et al.* 2012). In many instances, nulling has been observed across a wide frequency range making it a broadband phenomenon (even though the exact value of NF reported appears to have large variation over observing frequencies). This is strongly suggestive of intrinsic changes being responsible for nulling rather than geometrical effects. Not surprisingly, many subscribe to the thought that nulling is of magnetospheric origin (Kramer *et al.* 2006b; Wang *et al.* 2007; Lyne *et al.* 2010).

Therefore, it is important to look at the overall characteristics of the population of nulling pulsars in an effort to understand the origin of the phenomenon. A comprehensive list of nulling pulsars has recently been generated by Gajjar (2017) comprising of 109 objects. For the present work, we have done an extensive literature survey to extend and update that list. The number of nulling pulsars now stands at (likely more than) 204 (Tables 2–8). It goes without saying that, like any such list, this one is incomplete. Future observations would continue to add new nulling pulsars to this list, which may even exhibit hitherto unobserved characteristic features. However, the current size of nulling pulsar population is such that it allows us to draw certain broad conclusions about this sub-population of the larger class of RPP. In this work, we examine the distribution of NF and its correlation (or absence thereof)

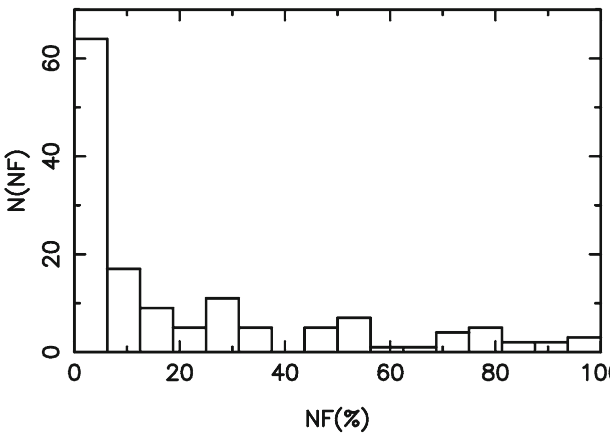

Figure 1. Histogram showing the distribution of NF, as available in the literature. Details can be found in Tables 1–4.

with various pulsar parameters. We also examine the general characteristics of the nulling pulsar population and revisit the connection of age with nulling behaviour.

2. Characteristics of nulling pulsar population

Only about 8% of all known radio pulsars (∼2500) are known to exhibit nulling (Tables 2–8). Quite likely this fraction is much larger, as only a small number of radio pulsars are observed over long periods (or regularly) to detect nulling episodes. Also, short nulls (nulling episode lasting only for a few pulses) may not be detected in weak pulsars. 7 among these are known to belong to the class of Intermediate Pulsars. Moreover, there exist a significant number of nulling pulsars for which no estimate for NF is available (Tables 6–7). Nevertheless it is possible to draw certain broad conclusions about the population. In this context, finding a correlation of NF with an intrinsic pulsar parameter (spin-period, characteristic age, magnetic field etc.) has been very important (Ritchings 1976; Wang *et al.* 2007). Analysing 72 nulling pulsars (Biggs 1992) found the spin-period (P_s) to be directly proportional to NF, consistent with an earlier work by Ritchings (1976). Later, characteristic age (τ_c) was found to be correlated with NF (Wang *et al.* 2007). Cordes and Shannon (2008) have also reported of finding some correlation of the nulling phenomenon with small inclination angles (angle between the rotation and the magnetic axes). These observations led to the suggestion that older pulsars are harder to detect as they spend more time in their null state (Ritchings 1976) and that the phenomenon of nulling is associated with the advanced age of a pulsar.

We find, that the NF histogram (Figure 1) is suggestive of some kind of bunching at lower values of NF, and a likely separation of NF values at ∼ 40% (although the data size is too small to find any clear indication for two different NF populations). The general characteristics of the nulling population, as seen in Figure 2 is as follows

- $-0.5 \lesssim \log P_s \lesssim 0.5$;
- 10^{11} G $\lesssim B_s \lesssim 10^{13}$ G;
- 10^6 Yr $\lesssim \tau_c \lesssim 10^8$ Yr; and
- 10 pc.cm$^{-3} \lesssim DM \lesssim 10^3$ pc.cm^{-3}.

It is evident that there does not appear to be any correlation of NF with any of the intrinsic parameters as per present data. Pearson correlation coefficients (von Mises 1980) calculated to find the level of correlation of NF with various pulsars parameters, as seen in Table 1, clearly demonstrate this. This behaviour also appears to be the same for pulsars with high as well low values of NF.

From Figure 3, it can be seen that the earlier conjecture, that nulling is predominantly experienced by old radio pulsars with relatively smaller magnetic fields, appears to be ruled out by the current population.

Interestingly, the nature of the distribution of the intrinsic parameters appear to be very different for pulsars exhibiting high NF compared to those having low values of NF. A nominal Kolmogorov-Smirnov (KS) test (von Mises 1980) on the spin-period of nulling pulsars with higher and lower values of NF, yields $P_{KS} = 0.002$ and $D_{KS} = 0.322$, rejecting the null hypothesis that these two populations have the same underlying distribution. [Here P_{KS} indicates the probability that the two distributions are inherently similar (identical), whereas D_{KS} is the maximum value of the absolute difference between the two distributions.] This is also evident from the fractional plot of period distributions shown in Figure 4.

3. Pulsar death-lines

Clearly, the nature of the emission mechanism must have a bearing on the nulling behaviour, whether or not nulling is directly related to the age of a pulsar. As mentioned earlier, Ritchings (1976) undertook the first comprehensive study of nulling pulsars and suggested that the time interval between regular bursts of pulse emission increases with age, eventually leading to pulsar 'death'. This study explicitly defined, for the very first time, a cut-off line for pulsar emission. This can be thought of as the precursor of more formal 'death-line's to be developed afterwards. Later, Zhang *et al.* (2007) also suggested that nulling pulsars are likely to be very close to the death line, being active only when favourable conditions prevail.

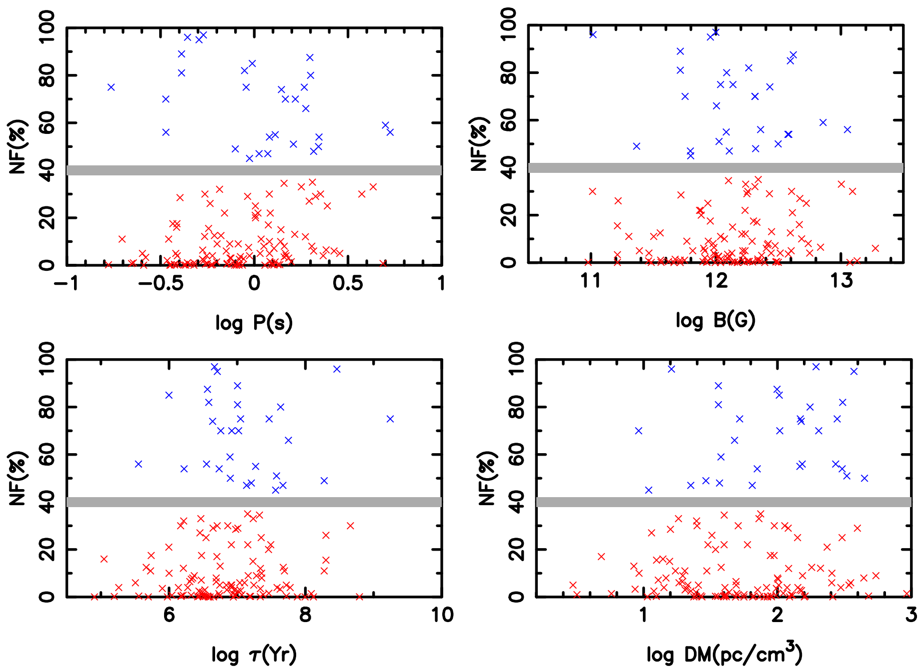

Figure 2. Variation of the nulling fraction (NF) against spin-period (P_s), surface magnetic field (B_s), characteristic age (τ_c) and dispersion measure (DM) of pulsars. The red points correspond to pulsars with low NF (< 40%) and the blue points to pulsars with larger values of NF. The horizontal grey band highlights the apparent gap in NF values around 40%.

Table 1. Pearson's correlation coefficient (r_P) for NF with various intrinsic pulsar parameters and the significance level (σ) of the calculated value of r_P.

		r_P	σ
NF > 40%	NF−P_s	−0.403	0.027
	NF−B_s	−0.220	0.242
	NF−$\dot{P}$	−0.119	0.528
	NF−τ_c	−0.047	0.807
	NF−DM	0.117	0.537
NF < 40%	NF−P_s	0.327	0.0004
	NF−B_s	0.134	0.160
	NF−$\dot{P}$	0.030	0.751
	NF−τ_c	0.100	0.295
	NF−DM	−0.017	0.861
ALL	NF−P_s	0.171	0.044
	NF−B_s	−0.020	0.813
	NF−$\dot{P}$	−0.091	0.283
	NF−τ_c	0.168	0.047
	NF−DM	0.180	0.033

[P_s – spin-period, B_s – derived surface magnetic field, $\dot{P}$ – spin-period derivative, τ_c – characteristic age, DM – dispersion measure].

Irrespective of the underlying mechanism, copious pair production in the magnetosphere is understood to be the basic requirement for pulsar emission. Such pair production gives rise to a dense plasma that can then allow the growth of a number of coherent instabilities and generate highly relativistic secondary pairs which then produce the radio band emission (see Mitra *et al.* 2009; Melrose 2017 and references therein for details of and recent progresses made in the area of pulsar emission physics).

Pulsars 'switch off' when conditions for pair production fail to be met. Depending on the specific model, radio pulsar 'death line' is defined to be a relation between P_s & $\dot{P}$ (period derivative) or P_s & B_s beyond which the process of pair-production ceases and a pulsar stops emitting. A number of theoretical models, consequently a variety of death-lines have been proposed to explain the present crop of pulsars. All of these require some degree of anomalous field configuration (higher multipole components or an offset dipole) to interpret the data in its entirety. Some of the most representative death-lines, based upon different models of emission mechanism, are described below.

In the following equations, B_p is the dipolar field, B_s is the surface field, r_c is the radius of curvature for the magnetic field, h is the thickness of the polar cap gap, R is the stellar radius and Ω is the stellar spin frequency. The value of inclination angle chosen for **5b** corresponds to that for Geminga.

A. Chen and Ruderman (1993):

I. Polar Cap Model: Pair production ($\gamma + B \rightarrow e^- + e^+$) predominantly happens near the polar cap of the neutron star (Ruderman & Sutherland 1975).

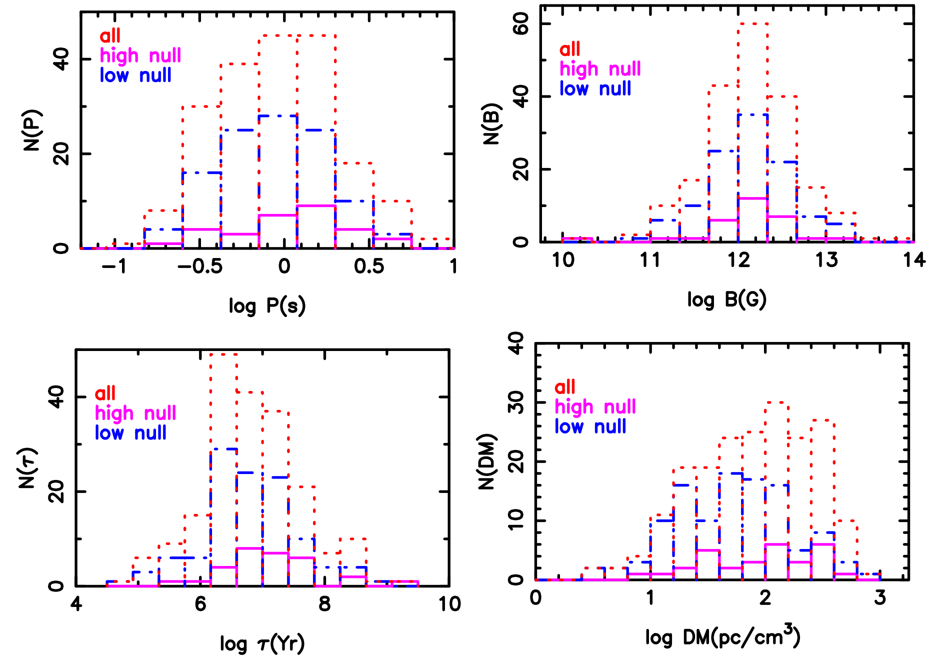

Figure 3. Distribution of characteristic pulsar parameters for pulsars with high null (NF < 40%), with low null (NF > 40%), and all of the nulling pulsars. It is to be noted that the histogram for all nulling pulsars also include pulsars without any estimate for NF and the intermittent pulsars.

01. Central Dipole, with $B_s = B_p$, $r_c = (Rc/\Omega)^{1/2}$ -

$$4 \log B - 7.5 \log P = 49.3, \quad (1)$$

01a. Dipole, off-centre by a distance d -

$$4 \log B - 7.5 \log P = 49.3 - 2.5 \log[R/(R-d)], \quad (2)$$

02. Very curved field lines, with $r_c \sim R$, $B_s = B_p$ -

$$4 \log B - 6.5 \log P = 45.7, \quad (3)$$

03. Very curved field lines, with $r_c \sim R$, $B_s = 2 \times 10^{13}$ G, $h \sim (B_p/B_s)^{1/2} R (R\Omega/c)^{1/2}$ at polar cap -

$$7 \log B - 13 \log P = 78, \quad (4)$$

04a, 04b. Extremely twisted field lines, with $r_c \sim R$ -

$$4 \log B - 6 \log P = 43.8 \text{ or } 31.3, \quad (5)$$

(Whichever constant produces larger B in the equation above to ensure $E_p > 2m_e c^2$.)

II. Outer Magnetospheric Model: Pair production happens in the outer magnetosphere via inverse Compton scattering, curvature radiation or synchrotron radiation etc.

05a, 05b. Aligned/Non-Aligned Dipole

$$5 \log B - 12 \log P = 72 \text{ or } 69.5. \quad (6)$$

B. Zhang *et al.* (2000): In each of the pair of equations below (depicted by the sets **06a-06b, 07a-07b, 08a-08b, 09a-09b**), the first one corresponds to a dipole configuration and the second one corresponds to a multipolar configuration with $B_s \sim B_p$ and $r_c \sim R$. Furthermore, r_{c6} is r_c in units of 10^6 cm.

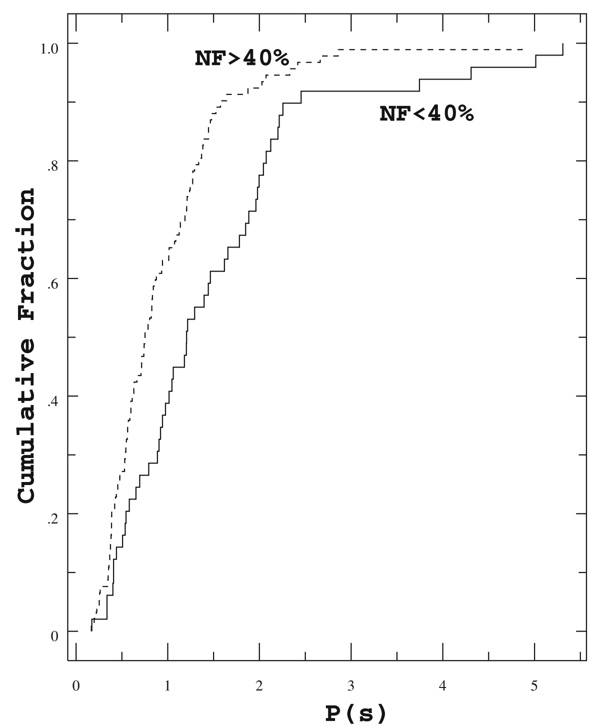

Figure 4. Cumulative fraction plot for the P_s distribution of pulsars with low (< 40%) and high (> 40%) values of NF.

I. Vacuum Gap Model: Pair production happens via formation of a vacuum gap close to the polar cap.

A. Curvature Radiation

06a. $\log \dot{\mathrm{P}} = 11/4 \log P - 14.62,$ (7)

06b. $\log \dot{\mathrm{P}} = 9/4 \log P - 16.58 + \log r_{c6},$ (8)

B. Inverse Compton Scattering

07a. $\log \dot{\mathrm{P}} = 2/11 \log P - 13.07,$ (9)

07b. $\log \dot{\mathrm{P}} = -2/11 \log P - 14.50 + 8/11 \log r_{c6},$ (10)

II. Space-Charge Limited Flow Model: If charged particles can be freely pulled out of the neutron star surface, a space-charged limited flow is generated. Mechanisms similar to those above then work to generate secondary/tertiary pairs.

A. Curvature radiation

08a. $\log \dot{\mathrm{P}} = 5/2 \log P - 14.56,$ (11)

08b. $\log \dot{\mathrm{P}} = 2 \log P - 16.52 + \log r_{c6},$ (12)

B. Inverse Compton Scattering -

09a. $\log \dot{\mathrm{P}} = -3/11 \log P - 15.36,$ (13)

09b. $\log \dot{\mathrm{P}} = -7/11 \log P - 16.79 + 8/11 \log r_{c6}.$ (14)

All the death-lines discussed above have been indicated in the top panel of Figure 5, in the backdrop of the known radio pulsars in $\mathrm{P_s}$-$\mathrm{B_s}$ plane. It should be noted that while the death lines are defined in terms of the magnetic field by Chen and Ruderman (1993), they are defined using the derivative of spin-period ($\dot{\mathrm{P}}$) by Zhang *et al.* (2000). However, the magnetic field is not a measured quantity. An estimate, only for the dipolar component, is obtained from the measured quantities $\mathrm{P_s}$ and $\dot{\mathrm{P}}$ through the following relation (Manchester & Taylor 1977)

$$B_{\mathrm{p}} \simeq 3.2 \times 10^{19} \left(\frac{P_s}{s}\right)^{\frac{1}{2}} \left(\frac{\dot{\mathrm{P}}}{ss^{-1}}\right)^{\frac{1}{2}} \mathrm{G}\,. \quad (15)$$

In Figure 5, this measure of the magnetic field is used for known pulsars. The death-line equations, given in terms of $\mathrm{P_s}$ and $\dot{\mathrm{P}}$ by Zhang *et al.* (2000), are also plotted in the $\mathrm{P_s}$-$\mathrm{B_s}$ plane using the same measure. Therefore, any conclusion drawn for this set of death-line equations do not suffer from an ambiguity regarding the measure of the magnetic field (between the dipolar and the true surface field). However, that is not correct in case of the death-lines defined by Chen and Ruderman (1993), which suffer from this ambiguity. It is clear that the death-lines **7a-7b, 9a-9b** are not very useful in constraining the radio pulsar population. In particular, they completely fail to accommodate the millisecond pulsars. Even if one questions whether the same death-line works for both the ordinary and millisecond pulsars, because these equations also preclude a significant number of relatively low field pulsars, we shall not consider them hereafter. On the other hand, the death-line depicted by **4b** is far too deep into the 'graveyard' to be of much use for the current population of pulsars. Perhaps the newly discovered long-period pulsars (some of which have been indicated by red stars in the bottom panel of Figure 5) are likely to be constrained by this equation. Among the rest, **1, 6a** and **2, 6b** are pairwise coincident (almost); while **2, 3** and **4** envelope somewhat similar regions. (**8a, 8b** are, more or less, coincident with **6a, 6b** and therefore not shown in the figure.)

In the bottom panel of Figure 5 the nulling pulsars (along with intermediate pulsars) are shown along with a relevant subset of death-lines. A number of (non-nulling) pulsars have been also been identified for their importance in the context of death-lines. For example, despite the wide variety of models and the large number of possible death-lines described above, it was necessary to invoke higher multipoles, many orders of magnitude stronger than the dipole, at the the surface to accommodate the 8.5 s pulsar J2144-3933 Gil and Mitra (2001). Other pulsars, like J1232-3933 (Jacoby *et al.* 2009), J1333-4449 (Jacoby *et al.* 2009) or J2123+5454 (Stovall *et al.* 2014) may also have similar explanations for them to work beyond the death-line **4a**. It is to be noted that J0250+5854 (Tan *et al.* 2018), the famous slow pulsar ($\mathrm{P_s} = 23.5$s), is actually within the allowed-zone, as far as death-lines are concerned.

It is likely that more than one emission mechanism could be responsible for radio pulsars activity (Chen and Ruderman 1993). It is then plausible that different death-lines are appropriate for pulsars in which different mechanisms are responsible for the emission. Though, at present, there is no clear understanding of this. However, when the population of nulling pulsars are marked out in the $\mathrm{P_s}$-$\mathrm{B_s}$ plane, certain remarkable things are noticed. It can be seen from the bottom panel of Figure 5 that there are almost no nulling pulsar above the death-line **5b** (definitely none above **5a**). Now, **5a, 5b** correspond to pure dipolar field configurations (aligned or non-aligned with the rotation axis) in an outer magnetospheric model. Given the current understanding of pulsar emission process, this may mean that the nulling pulsars likely do not possess purely dipolar field configurations where emission originates in the outer magnetosphere. On the other hand, the nulling pulsars appear to be bounded below by death-line **2**, which corresponds to a polar cap emission model with very

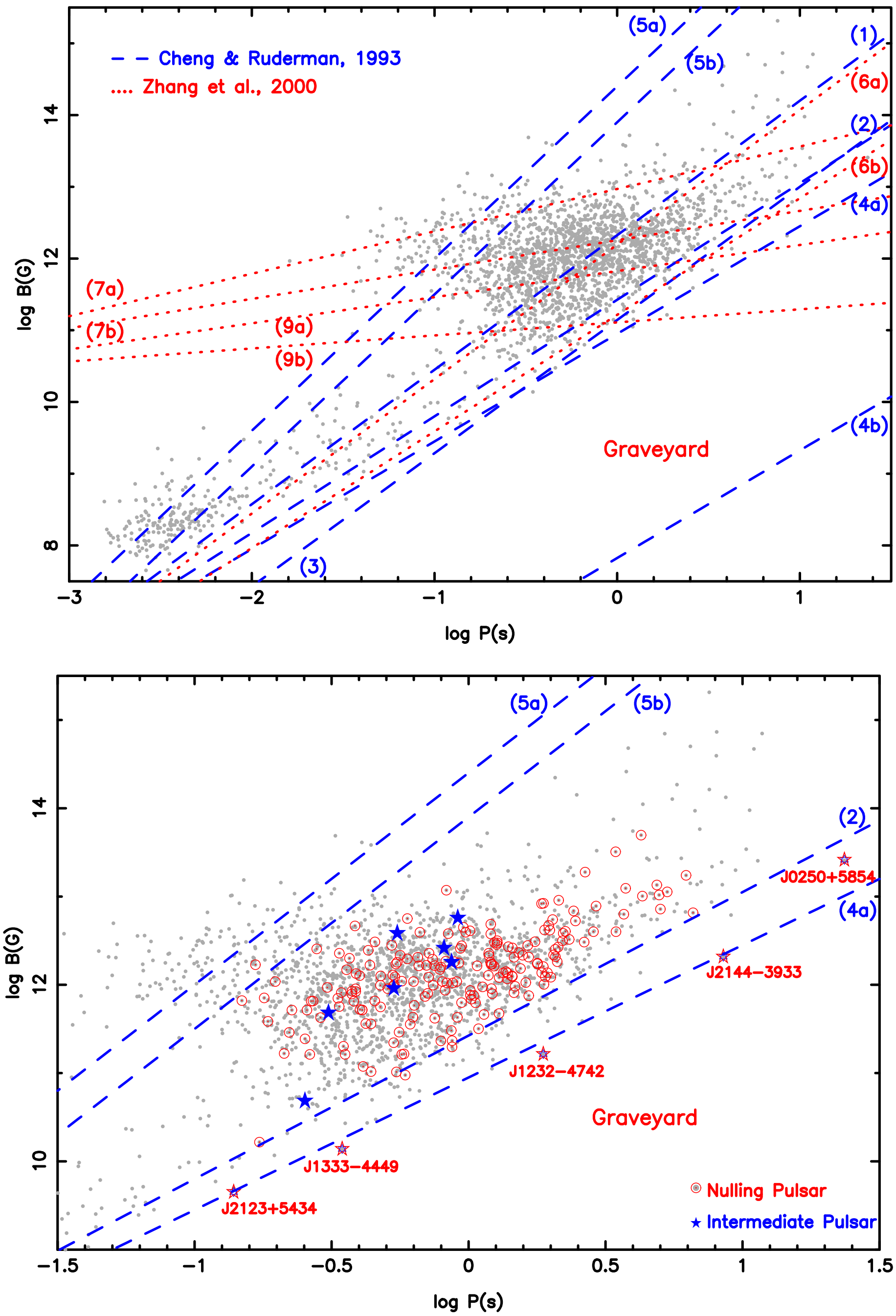

Figure 5. Observed radio pulsars and theoretical death-lines in the P_s-B_s plane. Top Panel: The death lines have been marked according to their numbering in the text. Bottom Panel: Nulling pulsars and intermediate pulsars have been highlighted with a small subset of death-lines. A number of pulsars have been specially identified (red open star) which appear to be functioning beyond the least stringent death line. The data for the known pulsars have been obtained from the ATNF pulsar catalog - http://www.atnf.csiro.au/research/pulsar/psrcat/ (Manchester *et al.* 2005).

curved field lines (curvature radius ∼ stellar radius). Taken together, it is suggestive of the conclusion that the pulsars for which the emission is predominantly from the polar cap and the magnetic field is extremely curved are likely to experience nulling episodes.

It has been suggested that in some pulsars, the magnetosphere may occasionally switch (‘mode change’) between different states with different geometries or/and different distributions of currents (Timokhin 2010). These states have different spin-down rates and emission beams; and some of the states do not (or apparently not) have any radio emission. In case of the intermittent pulsar, B1931+24, it has been clearly seen that $\dot{P}$ significantly differs from the off-state (nulling phase) to the on-state (active phase). It has been argued that, in the off-phase, the open field lines above the magnetic pole become depleted of charged particles and the rotational slow down happens purely due to the magnetic dipole radiation. On the other hand, in the on-phase, an additional slow-down torque is provided by the out-flowing plasma (Kramer *et al.* 2006a). Therefore, an estimate of the dipolar magnetic field obtained from measurements made during the active phase is always an overestimate. On the other hand, Young *et al.* (2012) has reported to have observed no change in the spin-down rate for the pulsar B0823+26 between the off-state and the on-state. This implies that there would be no overestimate of the dipolar field for this pulsar. Given this, it is difficult to gauge whether the reported values of $\dot{\mathrm{P}}$ and hence that of the dipolar field is an overestimate or not. However, even with a 10% overestimate (assumed for all the nulling pulsars), we find that our conclusions drawn above remain unchanged.

It is clear from the bottom-panel of Figure 5 that quite a large number of pulsars are active beyond the death-line **2**, but are bounded by the death-line **4a** which again corresponds to polar-cap emission but the magnetic field configurations for this case are extremely twisted. Because the pulsars in this region (between death-lines **2** and **4a**) are slow objects with no apparent significance they have mostly not been studied in detail. To our knowledge, there does not exist any study that specifically investigates the nulling behaviour of pulsars in this region. However, it is quite clear that if these objects are carefully monitored, for the presence of any nulling episodes, we would be able to gauge the validity of the conclusion above. With this in mind, we are initiating such a program, of targeted observation of slow pulsars between the death-lines **2** and **4a**, with the Giant Meterwave Radio Telescope (Konar *et al.* 2019).

4. Summary

About 8% of all known radio pulsars have been observed to exhibit nulling. In this work, we have considered NF to be the marker (for want of any other characteristic parameter which has been estimated for a significant number of nulling pulsars) for a pulsar's nulling behaviour and have looked at the nature of its distribution. We have also considered the general characteristics (in terms of intrinsic pulsar parameters) of this sub-population of radio pulsars. The conclusions drawn are summarised as follows

1. There appears to be a gap in the estimated value of nulling fraction around 40%, separating pulsars into two populations exhibiting higher and lower values of NF. However, this should be taken with a bit of caution, as inaccurate estimates of NF and inadequate study of pulsars with NF near 40% could contribute to this bias. On the other hand, the error bars, even though these could be quite large on occasion (Tables 2–5), do not appear likely to smudge out the gap.
2. The number of pulsars with a lower value (<40%) of NF appear to be far more in comparison to the ones with a higher value of NF (Figure 1). Once again, this could simply be an artifact of observational bias. For example, pulsars with very high NF are quite likely to be entirely missed by rapid pulsar surveys where other pulsars with zero (or small) nulling fractions are detected easily.
3. The distributions of the intrinsic pulsar parameters ($\mathrm{P_s}$, $\dot{\mathrm{P}}$, $\mathrm{B_s}$, τ_c, DM etc.) are statistically different in these two populations of pulsars with high and low values of NF.
4. There is no evidence of any correlation of NF with any of the intrinsic pulsar parameters as per present data. This behaviour is similar for pulsars with high as well as low values of NF.
5. The most interesting conclusion of our study is regarding the nature of the nulling pulsars. It appears likely that pulsars, for which the emission is predominantly from the polar cap and have extremely curved magnetic fields, preferentially experience nulling episodes. If borne out by future observations, this would pave the way for a theory of nulling which has so far eluded us.
6. Regular and targeted monitoring of pulsars in the region close to and bounded by the death-lines **2** and **4a** is therefore of great importance. As mentioned earlier, we are initiating a study with this goal.

Acknowledgements

Most of this work had been carried out when SK was supported by a Grant (SR/WOS-A/PM-1038/2014) from DST, Government of India and UD was supported through the 'Indian Academies' Summer Research Fellowship Programme (2017)'. Work done by Devansh Agarwal (also as a part of another summer project) has been useful in sorting out certain preliminary issues. SK would also like to thank Avinash Deshpande, Yashwant Gupta, Vishal Gajjar and Bhal Chandra Joshi for helpful discussions. We also thank the anonymous referee for helping to improve the clarity of the manuscript significantly.

Appendix. Nulling pulsar parameters

Table 2. Characteristic parameters - spin-period (P_s), surface magnetic field (B_s) and nulling fraction (NF) of known nulling pulsars.

	PR'S name	J-Name	P_s (s)	B_s (G)	NF (%)	References
1	B0031−07	J0034−0721	0.9429	6.28×10^{11}	44.0 ± 1.0	Gajjar (2017)
2	B0045+33	J0048+3412	1.2171	1.71×10^{12}	21.0 ± 1.0	Redman and Rankin (2009)
3	B0148−06	J0151−0635	1.4647	8.15×10^{11}	≤ 5.0	Biggs (1992)
4	B0149−16	J0152−1637	0.8327	1.05×10^{12}	≤ 2.5	Vivekanand (1995)
5	B0301+19	J0304+1932	1.3876	1.36×10^{12}	10.0	Rankin (1986)
6	B0329+54	J0332+5434	0.7145	1.22×10^{12}	≤ 0.25	Ritchings (1976)
7	B0450−18	J0452−1759	0.5489	1.80×10^{12}	≤ 0.5	Ritchings (1976)
8	J0458−0505	J0458−0505	1.8835	1.01×10^{12}	63.0 ± 3.0	Lynch *et al.* (2013)
9	B0523+11	J0525+1115	0.3544	1.63×10^{11}	≤ 0.06	Weisberg *et al.* (1986)
10	B0525+21	J0528+2200	3.7455	1.24×10^{13}	25.0 ± 5.0	Ritchings (1976)
11	B0529−66	J0529−6652	0.9757	3.94×10^{12}	83.5 ± 1.5	Crawford *et al.* (2013)
12	B0626+24	J0629+2415	0.4766	9.87×10^{11}	≤ 0.02	Weisberg *et al.* (1986)
13	B0628−28	J0630−2834	1.2444	3.01×10^{12}	≤ 0.3	Biggs (1992)
14	B0656+14	J0659+1414	0.3849	4.66×10^{12}	12.0 ± 4.0	Weisberg *et al.* (1986)
15	B0736−40	J0738−4042	0.3749	7.88×10^{11}	≤ 0.4	Biggs (1992)
16	B0740−28	J0742−2822	0.1668	1.69×10^{12}	≤ 0.2	Biggs (1992)
17	B0751+32	J0754+3231	1.4423	1.26×10^{12}	34.0 ± 0.5	Weisberg *et al.* (1986)
18	B0809+74	J0814+7429	1.2922	4.72×10^{11}	≤ 5.0	Ritchings (1976)
19	B0818−13	J0820−1350	1.2381	1.63×10^{12}	1.5 ± 0.25	Ritchings (1976)
20	B0818−41	J0820−4114	0.5454	1.03×10^{11}	30.0	Bhattacharyya *et al.* (2010)
21	B0820+02	J0823+0159	0.8649	3.04×10^{11}	≤ 0.06	Weisberg *et al.* (1986)
22	B0823+26	J0826+2637	0.5307	9.64×10^{11}	6.4 ± 0.8	Rankin and Rathnasree (1995)
23	B0826−34	J0828−3417	1.8489	1.37×10^{12}	75.0 ± 35.0	Durdin *et al.* (1979)
24	B0833−45	J0835−4510	0.0893	3.38×10^{12}	≤ 0.0008	Biggs (1992)
25	B0834+06	J0837+0610	1.2738	2.98×10^{12}	7.1 ± 0.1	Ritchings (1976)
26	B0835−41	J0837−4135	0.7516	1.65×10^{12}	1.7 ± 1.2	Gajjar (2017)
27	B0906−17	J0908−1739	0.4016	5.25×10^{11}	26.8 ± 1.7	Basu *et al.* (2017)
				5.25×10^{11}	25.7 ± 1.3	Basu *et al.* (2017)
28	B0919+06	J0922+0638	0.4306	2.46×10^{12}	≤ 0.05	Weisberg *et al.* (1986)
29	B0932−52	J0934−5249	1.4448	2.62×10^{12}	5.0 ± 3.0	Naidu *et al.* (2017)
30	B0940−55	J0942−5552	0.6644	3.94×10^{12}	≤ 12.5	Biggs (1992)
31	B0940+16	J0943+1631	1.0874	3.18×10^{11}	8.0 ± 3.0	Weisberg *et al.* (1986)
32	B0942−13	J0944−1354	0.5703	1.63×10^{11}	14.4 ± 0.9	Basu *et al.* (2017)
					≤ 7.0	Vivekanand (1995)
33	B0950+08	J0953+0755	0.2531	2.44×10^{11}	≤ 5.0	Ritchings (1976)
34	J1049−5833	J1049−5833	2.2023	3.15×10^{12}	47.0 ± 3.0	Wang *et al.* (2007)
					47.0 ± 3.0	Yang *et al.* (2014)
35	B1055−52	J1057−5226	0.1971	1.09×10^{12}	≤ 11.0	Biggs (1992)
36	B1112+50	J1115+5030	1.6564	2.06×10^{12}	64.0 ± 6.0	Gajjar (2017)
37	B1114−41	J1116−4122	0.9432	2.77×10^{12}	3.3 ± 0.5	Basu *et al.* (2017)
38	B1133+16	J1136+1551	1.1879	2.13×10^{12}	15.0 ± 2.5	Ritchings (1976)
39	B1237+25	J1239+2453	1.3824	1.17×10^{12}	6.0 ± 2.5	Ritchings (1976)
					7.0 ± 3.0	Naidu *et al.* (2017)
40	B1240−64	J1243−6423	0.3885	1.34×10^{12}	≤ 4.0	Biggs (1992)

The P_s and B_s values are taken from the ATNF database (http://www.atnf.csiro.au/research/pulsar/psrcat/) while NF values have been indicated with appropriate references, inclusive of cases where different estimates have been reported by different groups.

Table 3. Continuation of Table 2.

	PSR name	J-Name	P_s (s)	B_s (G)	NF (%)	References
41	B1322−66	J1326−6700	0.5430	1.72×10^{12}	9.1 ± 3.0	Wang *et al.* (2007)
42	B1325−49	J1328−4921	1.4787	9.61×10^{11}	4.0	Basu *et al.* (2017)
43	B1358−63	J1401−6357	0.8428	3.80×10^{12}	1.6 ± 2.0	Wang *et al.* (2007)
44	B1426−66	J1430−6623	0.7854	1.49×10^{12}	≤ 0.05	Biggs (1992)
45	B1451−68	J1456−6843	0.2634	1.63×10^{11}	≤ 3.3	Biggs (1992)
46	J1502−5653	J1502−5653	0.5355	9.99×10^{11}	93.0 ± 4.0	Wang *et al.* (2007)
47	B1508+55	J1509+5531	0.7397	1.95×10^{12}	7.0 ± 2.0	Naidu *et al.* (2017)
48	J1525−5417	J1525−5417	1.0117	4.09×10^{12}	16.0 ± 5.0	Wang *et al.* (2007)
49	B1524−39	J1527−3931	2.4176	6.87×10^{12}	5.1 ± 1.3	Basu *et al.* (2017)
50	B1530+27	J1532+2745	1.1248	9.48×10^{11}	6.0 ± 2.0	Weisberg *et al.* (1986)
51	B1530−53	J1534−5334	1.3689	1.41×10^{12}	≤ 0.25	Biggs (1992)
52	B1540−06	J1543−0620	0.7091	7.99×10^{11}	4.0 ± 2.0	Naidu *et al.* (2017)
53	B1556−44	J1559−4438	0.2571	5.18×10^{11}	≤ 0.01	Biggs (1992)
					0.24	Basu *et al.* (2017)
54	B1604−00	J1607−0032	0.4218	3.64×10^{11}	≤ 0.1	Biggs (1992)
55	B1612+07	J1614+0737	1.2068	1.71×10^{12}	≤ 5.0	Weisberg *et al.* (1986)
56	J1634−5107	J1634−5107	0.5074	9.04×10^{11}	90.0 ± 5.0	Young *et al.* (2015)
57	J1639−4359	J1639−4359	0.5876	9.50×10^{10}	≤ 0.1	Gajjar (2017)
58	B1641−45	J1644−4559	0.4551	3.06×10^{12}	≤ 0.4	Biggs (1992)
59	B1642−03	J1645−0317	0.3877	8.41×10^{11}	≤ 0.25	Ritchings (1976)
60	J1648−4458	J1648−4458	0.6296	1.09×10^{12}	1.4	Wang *et al.* (2007)
61	J1649+2533	J1649+2533	1.0153	7.63×10^{11}	≤ 20.0	Redman and Rankin (2009)
62	B1658−37	J1701−3726	2.4546	5.29×10^{12}	14.0 ± 2.0	Yang *et al.* (2014)
					19.0 ± 6.0	Gajjar (2017)
63	J1702−4428	J1702−4428	2.1235	2.68×10^{12}	26.0 ± 3.0	Wang *et al.* (2007)
64	B1700−32	J1703−3241	1.2118	9.05×10^{11}	1.6 ± 0.4	Basu *et al.* (2017)
65	J1703−4851	J1703−4851	1.3964	2.70×10^{12}	1.1	Wang *et al.* (2007)
					74.0	Yang *et al.* (2014)
66	B1706−16	J1709−1640	0.6531	2.05×10^{12}	31.0 ± 2.0, 15.0	Naidu *et al.* (2018)
67	J1715−4034	J1715−4034	2.0722	2.53×10^{12}	≤ 6.0	Gajjar (2017)
68	B1713−40	J1717−4054	0.8877	1.83×10^{12}	77.0 ± 5.0	Young *et al.* (2015)
					≥ 95.0	Wang *et al.* (2007)
69	B1718−32	J1722−3207	0.4772	5.62×10^{11}	1.0 ± 1.0	Naidu *et al.* (2017)
70	J1725−4043	J1725−4043	1.4651	2.05×10^{12}	≤ 70.0	Gajjar (2017)
71	J1727−2739	J1727−2739	1.2931	1.21×10^{12}	52.0 ± 3.0	Wang *et al.* (2007)
72	B1727−47	J1731−4744	0.8298	1.18×10^{13}	≤ 0.1	Biggs (1992)
73	B1730−37	J1733−3716	0.3376	2.28×10^{12}	52.4 ± 3.5	Basu *et al.* (2017)
74	J1738−2330	J1738−2330	1.9788	4.16×10^{12}	85.1 ± 2.3	Gajjar (2017)
75	B1737+13	J1740+1311	0.8031	1.09×10^{12}	≤ 0.02	Weisberg *et al.* (1986)
76	B1738−08	J1741−0840	2.0431	2.18×10^{12}	30.0 ± 5.0	Gajjar *et al.* (2017)
					15.7 ± 1.7, 15.8 ± 1.4	Basu *et al.* (2017)
77	J1744−3922	J1744−3922	0.1724	1.65×10^{10}	≤ 75.0	Faulkner *et al.* (2004)
78	B1742−30	J1745−3040	0.3674	1.99×10^{12}	≤ 17.5	Biggs (1992)
79	B1747−46	J1751−4657	0.7424	9.91×10^{11}	2.4 ± 0.5	Basu *et al.* (2017)
80	J1752+2359	J1752+2359	0.4091	5.19×10^{11}	≤ 89.0	Gajjar (2017)
81	B1749−28	J1752−2806	0.5626	2.16×10^{12}	≤ 0.75	Ritchings (1976)
82	J1752+2359	J1752+2359	0.4091	5.19×10^{11}	81.0	Yang *et al.* (2014)
83	B1758−03	J1801−0357	0.9215	1.77×10^{12}	27.7 ± 1.3, 26.1 ± 2.6	Basu *et al.* (2017)
84	J1808−0813	J1808−0813	0.8760	1.05×10^{12}	1.28 ± 1.3	Basu *et al.* (2017)
85	B1809−173	J1812−1718	1.2054	4.85×10^{12}	5.8 ± 0.4	Wang *et al.* (2007)

Table 4. Continuation of Tables 2 & 3.

	PSR name	J-Name	P_s (s)	B_s (G)	NF (%)	References
86	B1813−36	J1817−3618	0.3870	9.01×10^{11}	16.7 ± 0.7	Basu *et al.* (2017)
87	J1819+1305	J1819+1305	1.0604	6.25×10^{11}	41.0 ± 6.0	Yang *et al.* (2014)
88	B1818−04	J1820−0427	0.5981	1.97×10^{12}	≤ 0.25	Biggs (1992)
89	J1820−0509	J1820−0509	0.3373	5.67×10^{11}	67.0 ± 3.0	Wang *et al.* (2007)
90	B1819−22	J1822−2256	1.8743	1.61×10^{12}	10.0 ± 2.0	Naidu *et al.* (2017)
					4.7 ± 0.9	Basu *et al.* (2017)
					5.5 ± 0.7	−do−
91	B1821+05	J1823+0550	0.7529	4.18×10^{11}	≤ 0.4	Weisberg *et al.* (1986)
92	J1831−1223	J1831−1223	2.8580	3.99×10^{12}	4.0 ± 1.0	Wang *et al.* (2007)
93	J1833−1055	J1833−1055	0.6336	5.85×10^{11}	7.0 ± 2.0	Wang *et al.* (2007)
94	J1840−0840	J1840−0840	5.3094	1.13×10^{13}	50.0 ± 6.0	Gajjar *et al.* (2017)
95	B1839+09	J1841+0912	0.3813	6.52×10^{11}	≤ 5.0	Weisberg *et al.* (1986)
96	J1843−0211	J1843−0211	2.0275	5.48×10^{12}	6.0 ± 2.0	Wang *et al.* (2007)
97	B1842+14	J1844+1454	0.3755	8.48×10^{11}	≤ 0.15	Weisberg *et al.* (1986)
98	B1844−04	J1847−0402	0.5978	5.63×10^{12}	3.0 ± 1.0	Naidu *et al.* (2017)
99	B1845−19	J1848−1952	4.3082	1.01×10^{13}	27.0 ± 6.0	Naidu *et al.* (2017)
100	B1848+12	J1851+1259	1.2053	3.77×10^{12}	≤ 54.0	(Redman and Rankin 2009)
101	J1853+0505	J1853+0505	0.9051	1.09×10^{12}	67.0 ± 8.0	Young *et al.* (2015)
102	B1857−26	J1900−2600	0.6122	3.58×10^{11}	10.0 ± 2.5	Ritchings (1976)
103	J1901+0413	J1901+0413	2.6631	1.89×10^{13}	≤ 6.0	Gajjar (2017)
104	J1901−0906	J1901−0906	1.7819	1.73×10^{12}	29.0 ± 4.0	Naidu *et al.* (2017)
					2.9	Basu *et al.* (2017)
					5.6 ± 0.7	−do−
105	B1907+03	J1910+0358	2.3303	3.27×10^{12}	4.0 ± 0.2	Weisberg *et al.* (1986)
106	B1911−04	J1913−0440	0.8259	1.85×10^{12}	≤ 0.5	Ritchings (1976)
107	J1916+1023	J1916+1023	1.6183	1.06×10^{12}	47.0 ± 4.0	Wang *et al.* (2007)
108	B1917+00	J1919+0021	1.2723	3.16×10^{12}	≤ 0.4	Rankin (1986)
109	J1920+1040	J1920+1040	2.2158	3.83×10^{12}	50.0 ± 4.0	Wang *et al.* (2007)
110	B1918+19	J1921+1948	0.8210	8.68×10^{11}	9.0, 43.0	Rankin *et al.* (2013)
111	B1919+21	J1921+2153	1.3373	1.36×10^{12}	≤ 0.25	Ritchings (1976)
112	J1926−1314	J1926−1314	4.8643	1.35×10^{13}	$\sim 75.7 \pm 1.9$	Rosen *et al.* (2013)
113	B1923+04	J1926+0431	1.0741	1.64×10^{12}	≤ 5.0	Weisberg *et al.* (1986)
114	B1929+10	J1932+1059	0.2265	5.18×10^{11}	≤ 1.0	Ritchings (1976)
115	B1933+16	J1935+1616	0.3587	1.48×10^{12}	≤ 0.06	Biggs (1992)
116	B1942+17	J1944+1755	1.9969	1.22×10^{12}	≤ 60.0	Lorimer *et al.* (2002)
117	B1942−00	J1945−0040	1.0456	7.57×10^{11}	21.0 ± 1.0	Weisberg *et al.* (1986)
118	B1944+17	J1946+1805	0.4406	1.04×10^{11}	55.0 ± 5.0	Yang *et al.* (2014)
					64.0 ± 32.0	Ritchings (1976)
119	B1946+35	J1948+3540	0.7173	2.28×10^{12}	≤ 0.75	Ritchings (1976)
120	B2003−08	J2006−0807	0.5809	1.65×10^{11}	15.5 ± 1.0	Basu *et al.* (2017)
121	B2016+28	J2018+2839	0.5580	2.91×10^{11}	1.0 ± 3.0	Naidu *et al.* (2017)
122	B2020+28	J2022+2854	0.3434	8.16×10^{11}	0.2 ± 1.6	Gajjar (2017)
123	B2021+51	J2022+5154	0.5292	1.29×10^{12}	1.4 ± 0.7	Gajjar (2017)
124	J2033+0042	J2033+0042	5.0134	7.21×10^{12}	$44 - 49, 53 - 58$	Lynch *et al.* (2013)
125	B2034+19	J2037+1942	2.0744	2.08×10^{12}	44.0 ± 4.0	Herfindal and Rankin (2009)
					24.2 ± 1.5	−do−

Table 5. Continuation of Tables 2, 3 & 4.

	PSR name	J-Name	P_s (s)	B_s (G)	NF (%)	References
126	B2044+15	J2046+1540	1.1383	4.61×10^{11}	≤ 0.04	Weisberg *et al.* (1986)
127	B2045−16	J2048−1616	1.9616	4.69×10^{12}	22.0 ± 5.0	Naidu *et al.* (2017)
					5.5 ± 0.2	Basu and Mitra (2018)
128	B2053+36	J2055+3630	0.2215	2.89×10^{11}	≤ 0.7	Weisberg *et al.* (1986)
129	B2110+27	J2113+2754	1.2028	1.78×10^{12}	≤ 30.0	Redman and Rankin (2009)
130	B2111+46	J2113+4644	1.0147	8.62×10^{11}	21.0 ± 4.0	Gajjar (2017)
131	B2113+14	J2116+1414	0.4402	3.61×10^{11}	≤ 1.0	Weisberg *et al.* (1986)
132	B2122+13	J2124+1407	0.6941	7.39×10^{11}	≤ 22.0	Redman and Rankin (2009)
133	B2154+40	J2157+4017	1.5253	2.32×10^{12}	7.5 ± 2.5	Ritchings (1976)
134	J2208+5500	J2208+5500	0.9332	2.58×10^{12}	≤ 7.5	Joshi *et al.* (2009)
135	B2217+47	J2219+4754	0.5385	1.23×10^{12}	≤ 2.0	Ritchings (1976)
136	J2253+1516	J2253+1516	0.7922	2.32×10^{11}	≤ 49.0	Redman and Rankin (2009)
137	B2303+30	J2305+3100	1.5759	2.16×10^{12}	1.0	Rankin (1986)
138	B2310+42	J2313+4253	0.3494	2.01×10^{11}	≤ 11.0	Redman and Rankin (2009)
139	B2315+21	J2317+2149	1.4447	1.24×10^{12}	3.0 ± 0.5	Weisberg *et al.* (1986)
140	B2319+60	J2321+6024	2.2565	4.03×10^{12}	29.0 ± 1.0	Gajjar (2017)
141	B2327−20	J2330−2005	1.6436	2.79×10^{12}	12.0 ± 1.0	Biggs (1992)
142	J2346−0609	J2346−0609	1.1815	1.28×10^{12}	42.5 ± 3.8	Basu *et al.* (2017)
					28.7 ± 1.8	Basu *et al.* (2017)

Table 6. P_s and B_s of known nulling pulsars for which no NF estimates are available.

	PSR name	J-Name	P_s (s)	B_s (G)	References
1	J0229+20	J0229+20	0.8069	NA	Deneva *et al.* (2013)
2	J0726−2612	J0726−2612	3.4423	3.21×10^{13}	Burke-Spolaor *et al.* (2012)
3	B0853−33	J0855−3331	1.2675	2.86×10^{12}	Burke-Spolaor *et al.* (2012)
4	J0941−39	J0941−39	0.5868	NA	Burke-Spolaor and Bailes (2010)
5	J0943+2253	J0943+2253	0.5330	2.21×10^{11}	Brinkman *et al.* (2018)
6	J1012−5830	J1012−5830	2.1336	9.07×10^{12}	Burke-Spolaor *et al.* (2012)
7	J1055−6905	J1055−6905	2.9193	7.80×10^{12}	Burke-Spolaor *et al.* (2012)
8	B1056−57	J1059−5742	1.1850	2.28×10^{12}	Burke-Spolaor *et al.* (2012)
9	J1129−53	J1129−53	1.0629	NA	Burke-Spolaor *et al.* (2012)
10	B1131−62	J1133−6250	1.0229	6.88×10^{11}	Burke-Spolaor *et al.* (2012)
11	B1154−62	J1157−6224	0.4005	1.27×10^{12}	Burke-Spolaor *et al.* (2012)
12	J1225−6035	J1225−6035	0.6263	4.30×10^{11}	Burke-Spolaor *et al.* (2012)
13	J1255−6131	J1255−6131	0.6580	1.64×10^{12}	Burke-Spolaor *et al.* (2012)
14	J1307−6318	J1307−6318	4.9624	1.04×10^{13}	Burke-Spolaor *et al.* (2012)
15	B1323−58	J1326−5859	0.4780	1.26×10^{12}	Burke-Spolaor *et al.* (2012)
16	B1323−63	J1326−6408	0.7927	1.59×10^{12}	Burke-Spolaor *et al.* (2012)
17	J1406−5806	J1406−5806	0.2883	4.25×10^{11}	Burke-Spolaor *et al.* (2012)
18	J1423−6953	J1423−6953	0.3334	7.04×10^{11}	Burke-Spolaor *et al.* (2012)
19	B1424−55	J1428−5530	0.5703	1.10×10^{12}	Burke-Spolaor *et al.* (2012)
20	B1449−64	J1453−6413	0.1795	7.10×10^{11}	Burke-Spolaor *et al.* (2012)
21	B1454−51	J1457−5122	1.7483	3.08×10^{12}	Burke-Spolaor *et al.* (2012)
22	B1510−48	J1514−4834	0.4548	6.56×10^{11}	Burke-Spolaor *et al.* (2012)
23	J1514−5925	J1514−5925	0.1488	6.63×10^{11}	Burke-Spolaor *et al.* (2012)
24	B1555−55	J1559−5545	0.9572	4.48×10^{12}	Burke-Spolaor *et al.* (2012)

Table 6. continued

	PSR name	J-Name	P_s (s)	B_s (G)	References
25	J1624−4613	J1624−4613	0.8712	2.33×10^{11}	Burke-Spolaor *et al.* (2012)
26	B1630−44	J1633−4453	0.4365	1.67×10^{12}	Burke-Spolaor *et al.* (2012)
27	B1641−68	J1646−6831	1.7856	1.76×10^{12}	Burke-Spolaor *et al.* (2012)
28	J1647−3607	J1647−3607	0.2123	1.67×10^{11}	Burke-Spolaor *et al.* (2012)
29	J1649−4349	J1649−4349	0.8707	1.98×10^{11}	Burke-Spolaor *et al.* (2012)
30	B1650−38	J1653−3838	0.3050	9.33×10^{11}	Burke-Spolaor *et al.* (2012)
31	J1707−4729	J1707−4729	0.2665	6.53×10^{11}	Burke-Spolaor *et al.* (2012)
32	J1736−2457	J1736−2457	2.6422	3.05×10^{12}	Burke-Spolaor *et al.* (2012)
33	J1741−3016	J1741−3016	1.8938	4.18×10^{12}	Burke-Spolaor *et al.* (2012)
34	J1742−4616	J1742−4616	0.4124	1.19×10^{11}	Burke-Spolaor *et al.* (2012)
35	J1749+16	J1749+16	2.3117	NA	Deneva *et al.* (2016)
36	J1750+07	J1750+07	1.9088	NA	Deneva *et al.* (2016)
37	B1747−31	J1750−3157	0.9104	4.28×10^{11}	Burke-Spolaor *et al.* (2012)
38	J1757−2223	J1757−2223	0.1853	3.85×10^{11}	Burke-Spolaor *et al.* (2012)
39	J1758−2540	J1758−2540	2.1073	1.83×10^{12}	Burke-Spolaor *et al.* (2012)
40	B1806−21	J1809−2109	0.7024	1.66×10^{12}	Burke-Spolaor *et al.* (2012)
41	J1819−1458	J1819−1458	4.2632	5.01×10^{13}	Burke-Spolaor *et al.* (2012)
42	J1823−1126	J1823−1126	1.8465	8.31×10^{12}	Burke-Spolaor *et al.* (2012)
43	B1822−14	J1825−1446	0.2792	2.55×10^{12}	Burke-Spolaor *et al.* (2012)
44	J1827−0750	J1827−0750	0.2705	6.54×10^{11}	Burke-Spolaor *et al.* (2012)
45	J1830−1135	J1830−1135	6.2216	1.74×10^{13}	Burke-Spolaor *et al.* (2012)

Table 7. Continuation of Table 6.

	PSR name	J-Name	P_s (s)	B_s (G)	References
46	B1834−06	J1837−0653	1.9058	1.23×10^{12}	Burke-Spolaor *et al.* (2012)
47	J1837−1243	J1837−1243	1.8760	8.38×10^{12}	Burke-Spolaor *et al.* (2012)
48	J1840−1419	J1840−1419	6.5976	6.54×10^{12}	Burke-Spolaor *et al.* (2012)
49	J1841−0310	J1841−0310	1.6577	7.54×10^{11}	Burke-Spolaor *et al.* (2012)
50	J1852−0635	J1852−0635	0.5242	2.78×10^{12}	Burke-Spolaor *et al.* (2012)
51	J1854−1557	J1854−1557	3.4532	3.99×10^{12}	Burke-Spolaor *et al.* (2011)
52	J1857−1027	J1857−1027	3.6872	6.31×10^{12}	Burke-Spolaor *et al.* (2012)
53	J1935+1159	J1935+1159	1.9398	1.37×10^{12}	Brinkman *et al.* (2018)
54	B2043−04	J2046−0421	1.5469	1.53×10^{12}	Naidu *et al.* (2017)
55	J2050+1259	J2050+1259	1.2210	7.94×10^{11}	Brinkman *et al.* (2018)

Table 8. P_s and B_s of known Intermittent Pulsars.

	PSR name	J-Name	P_s (s)	B_s (G)	References
1	J1107−5907	J1107−5907	0.2528	4.83×10^{10}	Meyers *et al.* (2018)
2	J1832+0029	J1832+0029	0.5339	9.09×10^{11}	Lorimer *et al.* (2012)
3	J1839+15	J1839+15	0.5492	3.83×10^{12}	Surnis *et al.* (2013)
4	J1841−0500	J1841−0500	0.9129	5.80×10^{12}	Camilo *et al.* (2012)
5	J1910+0517	J1910+0517	0.3080	4.80×10^{11}	Lyne *et al.* (2017)
6	J1929+1357	J1929+1357	0.8669	1.80×10^{12}	Lyne *et al.* (2017)
7	B1931+24	J1933+2421	0.8137	2.60×10^{12}	Kramer *et al.* (2006a)

References

Backer D. C. 1970, Nature, 228, 42
Basu R., Mitra D. 2018, MNRAS, 476, 1345
Basu R., Mitra D., Melikidze G. I. 2017, ApJ, 846, 109
Bhattacharyya B., Gupta Y., Gil J. 2010, MNRAS, 408, 407
Biggs J. D. 1992, ApJ, 394, 574
Brinkman C., Freire P. C. C., Rankin J., Stovall K. 2018, MNRAS, 474, 2012
Burke-Spolaor S., Bailes M. 2010, MNRAS, 402, 855
Burke-Spolaor S. *et al.* 2011, MNRAS, 416, 2465
Burke-Spolaor S. *et al.* 2012, MNRAS, 423, 1351
Camilo F., Ransom S. M., Chatterjee S., Johnston S., Demorest P. 2012, ApJ, 746, 63
Chen K., Ruderman M. 1993, ApJ, 402, 264
Cordes J. M., Shannon R. M. 2008, ApJ, 682, 1152
Crawford F., Lorimer D., Ridley J., Madden J. 2013, in American Astronomical Society Meeting Abstracts, Vol. 221, American Astronomical Society Meeting Abstracts #221, p. 412.04
Deneva J. S. *et al.* 2016, ApJ, 821, 10
Deneva J. S., Stovall K., McLaughlin M. A., Bates S. D., Freire P. C. C., Martinez J. G., Jenet F., Bagchi M. 2013, ApJ, 775, 51
Deshpande A. A., Rankin J. M. 2001, MNRAS, 322, 438
Durdin J. M., Large M. I., Little A. G., Manchester R. N., Lyne A. G., Taylor J. H. 1979, MNRAS, 186, 39P
Dyks J., Zhang B., Gil J. 2005, ApJ, 626, L45
Esamdin A., Lyne A. G., Graham-Smith F., Kramer M., Manchester R. N., Wu X. 2005, MNRAS, 356, 59
Faulkner A. J. *et al.* 2004, MNRAS, 355, 147
Filippenko A. V., Radhakrishnan V. 1982, ApJ, 263, 828
Gajjar V. 2017, arXiv:1706.05407
Gajjar V., Joshi B. C., Kramer M. 2012, MNRAS, 424, 1197
Gajjar V., Joshi B. C., Kramer M., Karuppusamy R., Smits R. 2014, ApJ, 797, 18
Gajjar V., Yuan J. P., Yuen R., Wen Z. G., Liu Z. Y., Wang N. 2017, ApJ, 850, 173
Gil J., Mitra D. 2001, ApJ, 550, 383
Herfindal J. L., Rankin J. M. 2007, MNRAS, 380, 430
Herfindal J. L., Rankin J. M. 2009, MNRAS, 393, 1391
Jacoby B. A., Bailes M., Ord S. M., Edwards R. T., Kulkarni S. R. 2009, ApJ, 699, 2009
Johnston S., Lyne A. G., Manchester R. N., Kniffen D. A., D'Amico N., Lim J., Ashworth M. 1992, MNRAS, 255, 401
Joshi B. C. *et al.* 2009, MNRAS, 398, 943
Kaspi V. M. 2010, Proc. Natl. Acad. Sci. 107, 7147
Konar S. 2013, in Astronomical Society of India Conference Series, Vol. 8, Das S., Nandi A., Chattopadhyay I., eds, Astronomical Society of India Conference Series, p. 89
Konar S. 2017, J. Astrophys. Astronomy, 38, 47
Konar S. 2019, in prep
Konar S. *et al.* 2016, J. Astrophys. Astronomy, 37, 36
Konar S., Roy J., Bhattacharyaa B., 2019, in prep
Kramer M., Lyne A. G., O'Brien J. T., Jordan C. A., Lorimer D. R., 2006a. Science, 312, 549
Kramer M. *et al.* 2006b, Science, 314, 97
Li J., Esamdin A., Manchester R. N., Qian M. F., Niu H. B. 2012, MNRAS, 425, 1294
Lorimer D. R., Camilo F., Xilouris K. M. 2002, AJ, 123, 1750
Lorimer D. R., Lyne A. G., McLaughlin M. A., Kramer M., Pavlov G. G., Chang C. 2012, ApJ, 758, 141
Lynch R. S. *et al.* 2013, ApJ, 763, 81
Lyne A., Hobbs G., Kramer M., Stairs I., Stappers B. 2010, Science, 329, 408
Lyne A. G., McLaughlin M. A., Keane E. F., Kramer M., Espinoza C. M., Stappers B. W., Palliyaguru N. T., Miller J. 2009, MNRAS, 400, 1439
Lyne A. G. *et al.* 2017, ApJ, 834, 72
Manchester R. N., Hobbs G. B., Teoh A., Hobbs M. 2005, VizieR Online Data Catalog, 7245, 0
Manchester R. N., Taylor J. H. 1977, Pulsars. W. H. Freeman, San Francisco, San Francisco, p. 36
McLaughlin M. A. *et al.* 2006, Nature, 439, 817
Melrose D. B. 2017, Rev. Modern Plasma Phys., 1, 5
Meyers B. W. *et al.* 2018, ApJ, 869, 134
Mitra D., Gil J., Melikidze G. I. 2009, ApJ, 696, L141
Naidu A., Joshi B. C., Manoharan P. K., KrishnaKumar M. A. 2017, A&A, 604, A45
Naidu A., Joshi B. C., Manoharan P. K., Krishnakumar M. A. 2018, MNRAS, 475, 2375
O'Brien J. T., Kramer M., Lyne A. G., Lorimer D. R., Jordan C. A. 2006, Chin. J. Astronomy Astrophys. Suppl., 6, 4
Rajwade K., Gupta Y., Kumar U., Arjunwadkar M. 2014, in Astronomical Society of India Conference Series, Vol. 13, Astronomical Society of India Conference Series, p. 73
Rankin J. M. 1986, ApJ, 301, 901
Rankin J. M., Rathnasree N. 1995, J. Astrophys. Astronomy, 16, 327
Rankin J. M., Wright G. A. E. 2007, MNRAS, 379, 507
Rankin J. M., Wright G. A. E. 2008, MNRAS, 385, 1923
Rankin J. M., Wright G. A. E., Brown A. M. 2013, MNRAS, 433, 445
Redman S. L., Rankin J. M. 2009, MNRAS, 395, 1529
Ritchings R. T. 1976, MNRAS, 176, 249
Rosen R. *et al.* 2013, ApJ, 768, 85
Ruderman M. A., Sutherland P. G. 1975, ApJ, 196, 51
Stovall K. *et al.* 2014, ApJ, 791, 67
Surnis M. P., Joshi B. C., McLaughlin M. A., Gajjar V. 2013, in IAU Symposium, Vol. 291, IAU Symposium, p. 508
Tan C. M. *et al.* 2018, ApJ, 866, 54
Timokhin A. N. 2010, MNRAS, 408, L41
Vivekanand M. 1995, MNRAS, 274, 785
von Mises R. 1980, Mathematical Theory of Probability and Statistics. Academic Press, New York
Wang N., Manchester R. N., Johnston S. 2007, MNRAS, 377, 1383
Weisberg J. M., Armstrong B. K., Backus P. R., Cordes J. M., Boriakoff V., Ferguson D. C. 1986, AJ, 92, 621

Yang A., Han J., Wang N. 2014, Sci. China Phys. Mech. Astronomy, 57, 1600
Young N. J., Stappers B. W., Weltevrede P., Lyne A. G., Kramer M. 2012, MNRAS, 427, 114
Young N. J., Weltevrede P., Stappers B. W., Lyne A. G., Kramer M. 2014, MNRAS, 442, 2519
Young N. J., Weltevrede P., Stappers B. W., Lyne A. G., Kramer M. 2015, MNRAS, 449, 1495
Zhang B., Gil J., Dyks J. 2007, MNRAS, 374, 1103
Zhang B., Harding A. K., Muslimov A. G. 2000, ApJ, 531, L135